Applied and Environmental Microbiology, June 2008, p. 3764–3773 Vol. 74, No. 12
0099-2240/08/$08.00+0 doi:10.1128/AEM.00453-08

Insights into the Mode of Action of Chitosan as an Antibacterial Compound▽†

Dina Raafat,[1]* Kristine von Bargen,[2] Albert Haas,[2] and Hans-Georg Sahl[1]

Institute for Medical Microbiology, Immunology and Parasitology (IMMIP), Pharmaceutical Microbiology Unit, University of Bonn, D-53115 Bonn, Germany,[1] and Institute for Cell Biology, University of Bonn, D-53121 Bonn, Germany[2]

Received 25 February 2008/Accepted 22 April 2008

Chitosan is a polysaccharide biopolymer that combines a unique set of versatile physicochemical and biological characteristics which allow for a wide range of applications. Although its antimicrobial activity is well documented, its mode of action has hitherto remained only vaguely defined. In this work we investigated the antimicrobial mode of action of chitosan using a combination of approaches, including in vitro assays, killing kinetics, cellular leakage measurements, membrane potential estimations, and electron microscopy, in addition to transcriptional response analysis. Chitosan, whose antimicrobial activity was influenced by several factors, exhibited a dose-dependent growth-inhibitory effect. A simultaneous permeabilization of the cell membrane to small cellular components, coupled to a significant membrane depolarization, was detected. A concomitant interference with cell wall biosynthesis was not observed. Chitosan treatment of *Staphylococcus simulans* 22 cells did not give rise to cell wall lysis; the cell membrane also remained intact. Analysis of transcriptional response data revealed that chitosan treatment leads to multiple changes in the expression profiles of *Staphylococcus aureus* SG511 genes involved in the regulation of stress and autolysis, as well as genes associated with energy metabolism. Finally, a possible mechanism for chitosan's activity is postulated. Although we contend that there might not be a single classical target that would explain chitosan's antimicrobial action, we speculate that binding of chitosan to teichoic acids, coupled with a potential extraction of membrane lipids (predominantly lipoteichoic acid) results in a sequence of events, ultimately leading to bacterial death.

Chitosan, discovered by Rouget in 1859 (37), is a technologically important and ubiquitous polysaccharide biopolymer. It is produced by partial alkaline N deacetylation of chitin, which is commercially extracted from shrimp and crab shells. Chitosan is also found in nature, such as in the cell walls of fungi of the class *Zygomycetes* and in insect cuticles. Chemically, it is a high-molecular-weight linear polycationic heteropolysaccharide comprising copolymers of β-1,4-linked D-glucosamine and *N*-acetyl-D-glucosamine. The term chitosan describes a heterogenous group of polymers differing in molecular weight, viscosity, degree of deacetylation, pK_a, etc. (41, 43). Chitosan is commercially produced in different parts of the world (Japan, North America, Poland, Italy, Russia, Norway, and India) on a large scale (41). It has been estimated that up to 10^9 to 10^{10} tons of chitosan are annually produced in nature (33).

Much of the commercial interest in chitosan arises from the fact that it combines unique biological characteristics which allow for a wide range of applications, including biodegradability, biocompatibility, and nontoxicity. Its oral mean lethal dose in mice was found to be in excess of 16 g/day/kg of body weight, which is higher than that of sucrose (13, 41).

In spite of its abundance in nature, the commercial utilization of chitosan has been developed only over the last 2 decades; it has emerged as a new biomaterial for food (36), pharmaceutical (20, 41), medical (44, 53), textile (42), agricultural (12), and other industries, as well as for wastewater purification (1).

In recent years, chitosan and its derivatives have attracted much attention as antimicrobial agents against fungi, bacteria, and viruses and as elicitors of plant defense mechanisms (9, 28, 35). In fact, a number of commercial applications of chitosan benefit from its antimicrobial activity, including its use in food preservation (36), manufacture of wound dressings (44) and antimicrobial-finished textiles (42). The lack of understanding of how this industrially valuable biopolymer exerts its antibacterial activities led us to our more systematic study of its mechanism of action.

It is generally assumed that the cationic nature of chitosan ($pK_a = 6.3$), conveyed by the positively charged NH_3^+ groups of glucosamine, might be a fundamental factor contributing to its interaction with the negatively charged microbial cell surface, ultimately resulting in impairment of vital bacterial activities (19, 21, 28, 54). On the other hand, it is claimed that some of chitosan's characteristics, such as its water-binding capacity as well as its abilities to chelate trace metals and to interact with DNA, might shed some light on its antimicrobial mode of action (35).

The ambiguity regarding chitosan's mode of action prompted us to investigate, in more detail, the mechanisms underlying its antibacterial activities. Against this background, we attempted in this study to apply an array of techniques, including whole-cell assays, in vitro assays, and transcriptional response analysis, in search for possible molecular mechanisms by which chitosan might inhibit and kill bacteria. We demonstrated that the mode of action of chitosan is probably more complex than

* Corresponding author. Mailing address: Institute for Medical Microbiology, Immunology and Parasitology (IMMIP), Pharmaceutical Microbiology Unit, University of Bonn, Meckenheimer Allee 168, D-53115 Bonn, Germany. Phone: (49) 228 73 2113. Fax: (49) 228 73 5267. E-mail: draafat@uni-bonn.de.

† Supplemental material for this article may be found at http://aem.asm.org/.

▽ Published ahead of print on 2 May 2008.

TABLE 1. Strains used in this study, together with culture media and susceptibility to chitosan

Strain	Description	Culture medium[a]	Antimicrobial susceptibility		
			MIC (μg/ml)[b]		MBC (μg/ml)[b]
			24 h	48 h	
S. simulans 22	Indicator strain	CAMHB	2.0	3.9	3.9
		PYG	15.6	15.6	15.6
		B-broth	15.6	15.6	15.6
		CDM	125.0	125.0	>1,000.0
S. aureus SG511	Indicator strain, methicillin susceptible	CAMHB	23.4	23.4	62.5
		PYG	62.5	93.8	93.8
		B-broth	125.0	125.0	187.5
		CDM	500.0	750.0	>1,000.0
S. aureus SA113 strains					
SA113	ATCC 35556, wild type	CAMHB alone	84.8	84.8	84.8
SA113 Δ*ypfP*::*erm*	*ypfP* deletion mutant	CAMHB with 5 μg/ml Erm	224.0	224.0	232.6
SA113 Δ*tagO*::*erm*	*tagO* deletion mutant	CAMHB with 5 μg/ml Erm	471.6	545.5	602.3
SA113 Δ*ypfP*::*spc* Δ*tagO*::*erm*	Double-knockout mutant	CAMHB with 2.5 μg/ml Erm plus 150 μg/ml Spc	375.0	385.4	385.4
SA113 Δ*dltA*::*spc*	*dltA* mutant	CAMHB with 200 μg/ml Spc	0.9	0.9	0.9

[a] Abbreviations: CAMHB, BBL cation-adjusted Mueller-Hinton II broth (Becton, Dickinson & Co., Sparks, MD); PYG (peptone-yeast-glucose broth) (0.2% Bacto peptone, 0.2% yeast extract, 5 mM glucose, 10 mM KPO_4 buffer [pH 7]); B-broth (1% casein hydrolysate, 0.5% yeast extract, 0.05% K_2HPO_4, 10 mM glucose); CDM, chemically defined medium (46) with modifications (phosphate buffer was replaced with HEPES [13 g/liter], L-cysteine was omitted, and a lower glucose concentration [1 g/liter] was used); Erm, erythromycin; Spc, spectinomycin.

[b] Average of at least three determinations.

initially assumed, involving a number of events, that may ultimately lead to a killing process.

MATERIALS AND METHODS

Bacterial strains and culture conditions. Two well-characterized gram-positive standard laboratory strains, regularly used in the study of cationic antimicrobial peptides (AMPs), were used in this study: *Staphylococcus simulans* 22 and *Staphylococcus aureus* SG511 (4, 31, 38, 39). In addition, *Staphylococcus aureus* SA113 (ATCC 35556), together with some of its deletion mutants, were included in some investigations (Table 1). Unless otherwise noted, 50-ml cultures were grown aerobically in 100-ml flasks at 37°C, with shaking at 150 rpm (Certomat H; Sartorius, Göttingen, Germany), using a 5% (vol/vol) inoculum from an overnight starter culture. Deviant growth conditions are mentioned separately in the different experimental procedures. Stock cultures were maintained in standard I nutrient broth (Merck KGaA, Darmstadt, Germany) at −70°C as 40% glycerol suspensions. Working cultures were maintained on plates of standard I nutrient agar (Merck KGaA; indicator strains) or B-medium (1% tryptone, 0.5% yeast extract, 0.5% NaCl, 0.1% K_2HPO_4, 0.1% glucose, 12 g/liter agar) containing the appropriate antibiotic(s) if necessary (SA113 strains) at 4°C and subcultured fortnightly.

Preparation of chitosan stock solution. Low-molecular-weight chitosan (chitosan, 75 to 85% deacetylated), purchased from Sigma-Aldrich Chemie GmbH (Taufkirchen, Germany), has a reported molecular mass of 50 to 190 kDa. Its stock solution (1% [wt/vol] in 1% acetic acid) was sterilized by autoclaving at 121°C for 20 min and stored at 4°C for subsequent use.

MIC and MBC estimations. Values of the MIC were determined by a broth microdilution assay. Briefly, serial twofold dilutions of the antimicrobial agent were prepared in the appropriate culture medium in sterile 96-well round-bottom polystyrene microtiter plates (Greiner Bio-One GmbH, Frickenhausen, Germany). The strains were grown in the respective broth at 37°C to an optical density at 600 nm (OD_{600}) of 1 and subsequently diluted in the same medium to about 2×10^5 CFU/ml. Each well of the microtiter plate then received 100 μl of the inoculated medium, and the plates were incubated at 37°C for up to 48 h. The MIC was read as the least concentration of the antimicrobial agent that was sufficient to completely inhibit visible bacterial growth. The MICs of chitosan for the two indicator strains were determined under different culture conditions, including different media and in the presence of 5, 20, 50, and 100 μM metal ions (Fe^{2+} and Zn^{2+}). The media used were BBL cation-adjusted Mueller-Hinton II broth (CAMHB) (Becton, Dickinson & Co., Sparks, MD), peptone-yeast-glucose broth (PYG) (0.2% Bacto Peptone, 0.2% yeast extract, 5 mM glucose, 10 mM KPO_4 buffer [pH 7]), B-broth (1% casein hydrolysate, 0.5% yeast extract, 0.05% K_2HPO_4, 10 mM glucose), and chemically defined medium (CDM) as defined in reference 46 with modifications. The viable cell count in 20-μl aliquots of each well of the microtiter plates was determined, to assign the minimum bactericidal concentration (MBC), the lowest concentration reducing the bacterial inoculum by ≥99.9% within 24 h. Susceptibility tests were repeated at least three separate times to check the reproducibility of the results.

Bacterial killing assay. Cultures of the indicator strain *S. aureus* SG511 in CAMHB (around 1×10^7 CFU/ml) were incubated separately in the absence (control) and presence of different chitosan concentrations (0.5×, 1×, 2×, 5×, and 10× MIC) for a period of 24 h at 37°C. Samples of the bacterial cultures were removed at regular intervals to record survival counts, expressed as CFU/ml. The surviving $\log_{10}$ CFU/ml was plotted against time for each of the different chitosan concentrations. In addition, killing assays were performed using *S. simulans* 22 cultures at different physiological states.

Cell leakage assays. Potassium release from *S. simulans* 22 in response to exposure to different chitosan concentrations (5 to 60 μg/ml) was determined as previously described (5), using cultures of *S. simulans* 22 grown in CAMHB (with and without 10 mM glucose). Chitosan-induced leakage was expressed relative to the total amount of potassium release induced by the addition of 1 μM nisin, and K^+ efflux was calculated as a percentage (30).

Leakage of UV-absorbing cellular components from *S. simulans* 22 upon treatment with chitosan (20 μg/ml) was measured by growing the test strain in CAMHB to an OD_{600} of 0.5, harvesting and washing pellets, and then resuspending the cells in choline buffer (300 mM choline chloride, 30 mM morpholineethanesulfonic acid, 20 mM Tris [pH 6.5]). The absorbance of cell-free supernatants was measured at 260 nm over a period of 2 h. The percent absorbance was calculated with reference to a culture run in parallel and treated with nisin (1 μM) for 2 h, whereas the percent OD_{600} refers to the optical density of the test culture relative to that of the starting culture.

Leakage of proteins was determined by using the method of Lowry et al. (25). In addition, an electrophoretic separation of the protein samples was conducted using common sodium dodecyl sulfate-polyacrylamide gel electrophoresis by the method of Laemmli (24) with a 4% stacking gel and a 12% separating gel. Sodium dodecyl sulfate-polyacrylamide gel electrophoresis was conducted at a voltage of 90 to 120 V for 120 to 140 min, and the proteins were visualized with Coomassie brilliant blue R 250.

Estimation of membrane depolarization using [^{3}H]TPP$^+$. *S. simulans* 22 was grown in CAMHB to an OD_{600} of 1, harvested, and then resuspended 1:3 in fresh medium. [^{3}H]tetraphenylphosphonium bromide ([^{3}H]TPP$^+$) (30.0 Ci/mmol; GE Healthcare UK Ltd., England), a small lipophilic cation whose equilibrium

across the cytoplasmic membrane is indicative of membrane potential, was added to a final concentration of 1 μCi/ml of cell suspension. The cell culture was treated with chitosan (5× MIC), and then aliquots were filtered onto 0.2-μm-pore-size cellulose acetate membranes (Schleicher & Schuell, Dassel, Germany) and washed twice with 50 mM phosphate buffer (pH 7.0). The filters were dried, and the radioactivity was measured in Quickszint 100 (Zinsser Analytic, Frankfurt, Germany) in a Packard 1900CA liquid scintillation counter. The membrane potential was calculated as previously described (38).

Fluorometric membrane depolarization assay using DiBAC$_4$(3). *S. simulans* 22 was allowed to grow in CAMHB at 37°C until it reached an OD_{600} of 0.5. The cell suspension was incubated in the dark for 25 min with 1 μM of the membrane potential-sensitive fluorescent probe bis-(1,3-dibutylbarbituric acid) trimethine oxonol [DiBAC$_4$(3)] (Molecular Probes, Invitrogen, Karlsruhe, Germany) at room temperature. Chitosan was then added to final concentrations of 10 to 60 μg/ml. The change in the intensity of fluorescence emission of DiBAC$_4$(3) was monitored for 15 min, using an RF-5301PC series spectrofluorophotometer (Shimadzu Corporation, Kyoto, Japan) at excitation and emission wavelengths of 492 and 515 nm, respectively.

Inhibition of in vitro lipid II synthesis. The analytical lipid II assay was performed as previously described (5). Chitosan was added to the reaction mixture to achieve final concentrations of 67 and 267 μg/ml. After incubation of the reaction mixtures for 1 h at 30°C, lipids were extracted with the same volume of *n*-butanol–6 M pyridine acetate (2:1, vol/vol), pH 4.2. The extraction mixture was separated by thin-layer chromatography (60F254 silica plates; Merck), and the lipid spots on the silica gel plate were visualized by phosphomolybdic acid staining.

Assessment of liposomal permeabilization. Carboxyfluorescein (CF)- and K^+-loaded unilamellar liposomes containing the zwitterionic, neutral phospholipid 1,2-dioleoyl-*sn*-glycero-3-phosphocholine (DOPC) and the anionic phospholipid 1,2-dioleoyl-*sn*-glycero-3-[phospho-*rac*-(1-glycerol)] sodium salt (DOPG) (both purchased from Avanti Polar Lipids, Inc., Alabaster, AL) in a molar ratio of 1:1 [DOPC-DOPG (1:1)] were prepared as described by Bonelli et al. (5).

Chitosan-induced efflux of CF was determined as follows. CF-loaded vesicles were diluted in Tris-buffered saline (TBS) (10 mM Tris-HCl [pH 7.2], 0.85% [wt/vol] NaCl) to a final concentration of 25 μM phospholipid based on phosphorus. CF leakage upon the addition of various concentrations of chitosan (0.5 to 200 μg/ml) was monitored over 5 min at 520 nm (excitation at 492 nm) on a spectrofluorophotometer at room temperature. Leakage was expressed relative to the total amount of CF released after disruption of the liposomes by the addition of 20 μl of 20% Triton X-100.

Potassium leakage from liposomes was determined after diluting the K^+-loaded vesicles in choline buffer to a final concentration of 250 μM phospholipid based on phosphorus. Potassium efflux was monitored in the presence of various concentrations of chitosan (1 to 200 μg/ml). K^+ leakage was expressed relative to the total amount of potassium recorded after complete lysis of the liposomes through the addition of 46 μl of 30% octylglycoside.

Electron microscopic examination of chitosan-treated cells. Cultures of *S. simulans* 22 were grown in CAMHB to the early exponential phase and then split into two portions: one was treated with chitosan (10× MIC) and incubated at 37°C, while the other served as an untreated control. Aliquots of the control culture as well as the chitosan-treated culture (collected after 5, 20, and 60 min) were harvested (1,000 × *g*, 10 min, 4°C), and the bacterial pellets were washed once in Sørensen's phosphate buffer with sucrose (SPS) (25.4 mM KH_2PO_4, 24.6 mM Na_2HPO_4, 0.1 M sucrose) and then prefixed in SPS containing 3% (wt/vol) glutaraldehyde (4°C, 4 h). After the cells were harvested, the fixed cells were resuspended in SPS (12 to 18 h, 4°C). The collected cell pellets were washed in SPS and then in 0.1 M cacodylate buffer. Contrasting was done using 1.5% potassium ferricyanide and 1% (wt/vol) osmium tetroxide (2 h on ice), whereas fixation was achieved by resuspending the pellet carefully in 5% (wt/vol) uranyl acetate (2 h on ice). After resuspension in 1% tannic acid (30 min, 25°C), the pellet was dehydrated and stained as previously described (26). The samples were then viewed with a Philips CM 120 transmission electron microscope.

Preparation of total RNA. *S. aureus* SG511 was grown in CAMHB to an OD_{600} of 0.8. Culture aliquots were either treated with chitosan (15 μg/ml) for 20 min, or left untreated (control), and then collected and quickly stabilized by adding RNAprotect Bacteria Reagent (Qiagen, Hilden, Germany). Cell pellets were lysed in the presence of 300 μg lysostaphin (Dr. Petry Genmedics GmbH, Reutlingen, Germany), and total RNA was extracted using the *PrestoSpin* R kit (Molzym, Bremen, Germany), according to the manufacturer's instructions. RNA concentration and purity were assessed photometrically.

Reverse transcriptase labeling of mRNA into Cy3- and Cy5-labeled cDNA. The purified RNA samples (9 μg of total RNA) were reverse transcribed into cDNA using BioScript reverse transcriptase (Bioline, Luckenwalde, Germany), and the cDNAs were concomitantly labeled by incorporation of cyanine-labeled nucleotides (0.1 mM cyanine-3′-dCTP or cyanine-5′-dCTP; GE Healthcare UK Limited, United Kingdom). The labeled targets were purified using the MinElute PCR purification kit (Qiagen, Hilden, Germany), and the concentration of cDNA and the amount of incorporated dye were measured using the NanoDrop ND-1000 spectrophotometer (Peqlab, Erlangen, Germany).

Hybridization and data acquisition and analysis. The differentially labeled targets to be compared were combined and competitively hybridized (42°C, 72 h) to the custom *sciTRACER* full genome chip (Scienion AG, Berlin, Germany), containing 2,338 from all 2,593 protein-coding open reading frames (ORFs) in the annotated genome of *S. aureus* N 315, sequenced by Kuroda et al. (23). Washing and scanning of chips, image acquisition, and analysis of the scan data were carried out by the methods of Pag et al. (31).

Characterization of *S. aureus* SCVs. Hemin auxotrophy was tested by plating a culture of small-colony variants (SCVs) in CAMHB (10^4 CFU/ml) onto the surface of a BBL Mueller-Hinton II agar (MHA) plate (Becton, Dickinson & Co., Sparks, MD) and then aseptically transferring a hemin disc (Sigma-Aldrich Chemie GmbH) onto the center of the plate. As for thymidine and menadione auxotrophy, a diluted culture of SCVs in CAMHB was plated onto the surface of MHA plates, where cups were instilled with either thymidine (200 μg/well) or menadione (10 μg/well). The plates were incubated at 37°C for 24 to 48 h, and growth of the SCVs on all three plates was observed. To determine generation time, cultures (10^4 CFU/ml) of *S. aureus* SG511 and the SCVs were incubated at 37°C, and samples were withdrawn every 30 min (parent strain) or 90 min (SCVs) and plated on MHA plates for viable cell count determination. The plates were incubated at 37°C for 24 to 48 h (wild type) and for 48 to 72 h (SCVs). Moreover, conventional biochemical tests were used to compare both phenotypes.

TABLE 2. Characteristics of the chitosan sample used[a]

Sample or parameter	M_w (g/mol)	M_n (g/mol)	M_w/M_n	[η] (dl/g)	R_h (nm)	DD (%)
Chitosan	243.17	83.55	2.91	5.0	24.59	87
RSD (%)	1.5	13.4	11.7	1.5	1.4	2

[a] The molecular weight analysis was performed using size exclusion chromatography, and the detection was operated by a differential refractometer. Intrinsic viscosities were measured on a differential Wheatstone bridge viscometer. The degree of deacetylation was analyzed by ^{1}H nuclear magnetic resonance (Bruker Avance WB-360 [8.4-T] spectrometer). Abbreviations: M_w, weight-average molecular weight; M_n, number-average molecular weight; M_w/M_n, polydispersity; [η], intrinsic viscosity; R_h, hydrodynamic radius; DD, degree of deacetylation; RSD, relative standard deviation.

RESULTS

In vitro growth inhibition. Chitosan's antimicrobial activity varied against strains and was bacteriostatic, rather than bactericidal, judged by the slightly higher MBCs (Table 1). Since the antimicrobial activity of chitosan depends on a variety of factors, including its type (e.g., plain or derivative), molecular weight, and degree of deacetylation, we decided to subject chitosan to a detailed characterization (Table 2). The value of polydispersity (a measure for the width of the molar mass distribution of a polymer) indicated that the chitosan sample was quite heterogenous, encompassing polymers of widely ranging molecular weight distribution, thus explaining the occasional variation in MICs between determinations. Moreover, several chitosan samples with various molecular weights were found to be equally active against the tested strains. Taken together with the evidence that no significant difference in chitosan's activity was observed upon dialysis against acidulated water (Slide-A-Lyzer 10K dialysis cassette; Pierce, IL) for 48 h, it appears that molecules larger than 10 kDa were responsible for its activity. Therefore, we decided to use the characterized batch of chitosan for all subsequent experiments. The highest activity of chitosan was in CAMHB, with only

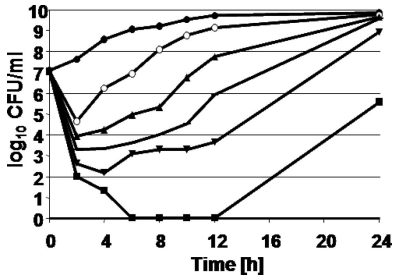

FIG. 1. Effect of chitosan on the growth kinetics of *S. aureus* SG511. Numbers of survivors (in log units) of *S. aureus* SG511 (starting inoculum of 1.15×10^7 CFU/ml) in CAMHB at 37°C in the presence of 0 (●), 0.5× (○), 1× (▲), 2× (—), 5× (▼), and 10× (■) MIC of chitosan.

residual activity in the other three media, probably due to the fact that it is insoluble in the presence of phosphate ions (Table 1). Divalent metal cations (Fe^{2+} and Zn^{2+}) reduced chitosan's antibacterial activity in a dose-dependent manner (data not shown), which is consistent with the chelating ability of chitosan toward transition metal salts in vitro (3).

Mode-of-action assays. Chitosan had a dose-dependent growth-inhibitory effect on *S. aureus* SG511 (Fig. 1). At 10× MIC, the number of surviving cells was drastically reduced within 6 h to below the detection limit. This apparent killing phase was, however, followed by regrowth, which might be attributed to the emergence of small-colony variants. SCVs constitute subpopulations of some *S. aureus* strains that are generally more resistant to the action of antimicrobials than their parent strain due to a decreased metabolism and a significantly reduced electrochemical gradient (2, 34). The parental strain (*S. aureus* SG511) demonstrated a typical *S. aureus* phenotype and was hemolytic on blood agar plates, whereas the SCV colonies were smaller, had an unstable colony phenotype, diminished hemolytic activity, decreased pigmentation and coagulase activity, delayed mannitol fermentation, slowed growth (doubling of generation time compared to that of the wild type), and were auxotrophic for menadione (data not shown). The SCV was less susceptible than the parent strain to chitosan, chloramphenicol, kanamycin, co-trimoxazole, rifampin, and oxacillin. Differences in MICs ranged from 1.5- to 30-fold, depending on the antimicrobial agent (Table 3). In-

TABLE 3. Susceptibility of *S. aureus* SG511 (parent strain) and its SCV to various antimicrobial agents

Antimicrobial agent	*S. aureus* SG511			SCV		
	MIC (μg/ml)[a]		MBC (μg/ml)[a]	MIC (μg/ml)[a]		MBC (μg/ml)[a]
	24 h	48 h		24 h	48 h	
Chitosan	23.4	23.4	31.3	15.6	187.5	250.0
Chloramphenicol	6.3	12.5		18.8	18.8	
Kanamycin	0.8	0.8		6.3	6.3	
Co-trimoxazole (trimethoprim-sulfamethoxazole)	2.0	2.0	4.0	2.0	4.0	>128.0
Rifampin	≤0.1	0.1	0.1	3.0	3.0	3.0
Oxacillin	0.4	0.5	0.5	0.6	1.1	2.1

[a] Results are the averages of two determinations.

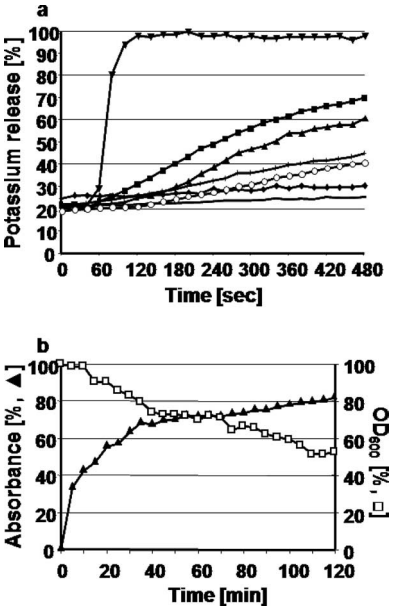

FIG. 2. Cell leakage assays. (a) Potassium release from *S. simulans* 22 cells (—) increases with increasing amounts of chitosan: 5 μg/ml (◆), 10 μg/ml (○), 20 μg/ml (+), 40 μg/ml (▲), and 60 μg/ml (■). 100% potassium leakage was achieved by the addition of 1 μM of the pore-forming lantibiotic nisin (▼). (b) Leakage of UV-absorbing cellular components from *S. simulans* 22, upon treatment with chitosan (20 μg/ml) in CAMHB, measured at 260 nm (▲). Nisin (1 μM) was used to mark 100% leakage. Parallel optical density measurements were conducted and compared to the initial culture density (percent OD_{600}, □).

terestingly, the addition of chitosan to *S. simulans* 22 cells in the stationary phase yielded lower viable cell counts than the same addition to cells in the late logarithmic phase.

We used a K^+-specific ion electrode to detect membrane impairment and leakage of cellular contents from *S. simulans* 22 cells after exposure to different concentrations of chitosan (5 to 60 μg/ml) in situ. Chitosan initiated a gradual, dose-dependent flux of K^+ ions from *S. simulans* 22, which was rather incomplete (Fig. 2a), compared to that of a pore-forming peptide, such as the lantibiotic nisin. However, preenergization of the cells in the presence of 10 mM glucose resulted in an accelerated K^+ efflux without influencing the extent of leakage. Moreover, treatment of *S. simulans* 22 cells with chitosan (20 μg/ml) resulted in a gradual leakage of UV-absorbing substances (likely representing nucleotide and coenzyme pools) from bacterial cells, followed by a plateau for up to 2 h (Fig. 2b). This leakage was also found to be concentration dependent. Optical density measurements of the treated culture revealed around 50% reduction in culture density after 2 h, which was attributed to aggregation and flocculation of the cells in the presence of chitosan. Attempts to detect protein leakage upon chitosan treatment failed, indicating that either no proteins leak out of the cells or they leak out in amounts too small to be detected. In sum, the leakage experiments uniformly indicated that chitosan efficiently permeabilized the plasma membranes of staphylococci for small cellular constituents. We aimed at extending these observations by investigating whether liposomes treated with chitosan became damaged

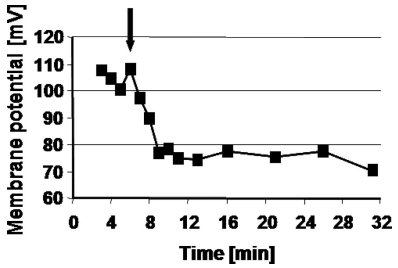

FIG. 3. Measurement of chitosan's ability to perturb the membrane potential ($\Delta\Psi$) using [^{3}H]TPP$^+$. Cells of *S. simulans* 22 in the late log phase were allowed to equilibrate with [^{3}H]TPP$^+$. Chitosan was then added (arrow) to a final concentration of 10 μg/ml.

and leaked trapped marker molecules. However, chitosan was unable to cause permeabilization of the negatively charged unilamellar DOPC-DOPG (1:1) liposomes to CF and K^+ ions (data not shown). These in vitro leakage assays served to illustrate that although chitosan might be endowed with considerable membrane permeabilization capacity when tested in vivo, it may be unable to effectively demonstrate a similar effect in an in vitro setting.

Perturbation of membrane integrity, by antimicrobials for instance, leads to membrane depolarization and ultimately bacterial cell death. In this study we found a substantial reduction in bacterial membrane potential $\Delta\Psi$ when we monitored the distribution of the small lipophilic charged [^{3}H]TPP$^+$ ions between cells of *S. simulans* 22 and the suspending medium in response to treatment with chitosan (Fig. 3). The depolarization kinetics were similar to the time course of potassium efflux. This contention was corroborated with the help of $DiBAC_4(3)$, a lipophilic and anionic fluorescent distributional probe, which accumulates only in cells in which the $\Delta\Psi$ is dissipated. With this probe, too, membrane depolarization was dose dependent (data not shown). Nevertheless, it was obvious that chitosan-induced depolarization was much slower and incomplete when compared to the antimicrobial peptide nisin (positive control).

Nisin is known to form a defined and stable pore, using the membrane-bound bacterial cell wall precursor lipid II as an anchor molecule, simultaneously resulting in inhibition of cell wall biosynthesis (50, 51). However, we were unable to detect such activity with chitosan in the in vitro lipid II assay (data not shown).

Examination of cell damage by transmission electron microscopy. To further understand chitosan's mode of action, we monitored ultrastructural changes of *S. simulans* 22 cells upon exposure to chitosan (10× MIC). Control cells showed an intact plasma membrane of high electron density and an outer cell wall of medium electron density which was more or less uniform along the entire cell perimeter; sites of cell division were also evident. Cells treated with chitosan for as short as 5 min showed irregular structures protruding from the cell surface, which might be chitosan deposits still attached to the negatively charged surface polymers (Fig. 4). Interestingly, it seemed that the cell membrane became locally detached from the cell wall, giving rise to "vacuole-like" structures underneath the cell wall, possibly resulting from ion and water efflux and decreased internal pressure. Nonetheless, the membrane was well discernible in all sections, i.e., was more or less physically intact. There was no evidence for cell wall lysis, as described for *S. simulans* 22 treated with the cationic peptides Pep5 and nisin, which activate cell wall-lytic enzymes from anionic cell wall polymers (4). Our electron microscopic findings thus did not support earlier work, which demonstrated an irregularly structured and frayed cell wall in chitosan-treated microorganisms (28), and even the appearance of protoplasts (10).

There was a fairly conspicuous nucleoid region of low density in both the control sample and in cells treated for 5 min (Fig. 4a and b, respectively); however, this region became more disperse and ill-defined in cells treated for 20 and 60 min (Fig. 4c and d, respectively), indicating that changes of the intracellular ionic milieu after the addition of chitosan might affect the bacterial nucleoid organization.

Influence of teichoic acids on the susceptibility of *S. aureus* to chitosan. Teichoic acids are essential polyanionic polymers of the cell walls of gram-positive bacteria, which appear to extend to the surface of the peptidoglycan layer. They can be either covalently linked to *N*-acetylmuramic acid of the peptidoglycan layer (wall teichoic acids) or anchored into the outer leaflet of the cytoplasmic membrane via a glycolipid (lipoteichoic acids [LTA]). To evaluate the possible involvement of teichoic acids of *S. aureus* in chitosan's antimicrobial activity and to analyze their role in chitosan susceptibility, we tested *S. aureus* strain SA113 together with four of its mutants lacking one or more genes involved in teichoic acid biosynthesis (Table 1).

S. aureus SA113 Δ*tagO* completely lacks wall teichoic acids due to deletion of the *tagO* gene which codes for an enzyme catalyzing the first step in the synthesis of wall teichoic acids (48). In the *ypfP* deletion mutant, the gene responsible for biosynthesis of the glycolipid anchor of LTA was absent, causing 87% reduction in LTA content compared to the LTA content in the wild type (14). A double mutant in which the *tagO* gene was replaced by an erythromycin cassette and the *ypfP* gene was replaced by a spectinomycin cassette was also available.

The *tagO* deletion mutant was the most resistant of the strains to the antimicrobial activity of chitosan (with more than fivefold-higher MIC), followed by the double mutant and the Δ*ypfP* mutant (Table 1). The relevance of this finding is significant, since the lack of teichoic acids in staphylococci results in a less negatively charged cell wall, further substantiating the hypothesis that the polycationic nature of chitosan is a major factor contributing to its antimicrobial activity. We believe the same reasoning can be applied to the fact that the Δ*dltA* mutant, which lacks the D-alanine modification in teichoic acids, as a result of which the cells carry an increased negative surface charge (32), was almost 100 times more susceptible to the action of chitosan, with an MIC as low as 0.9 μg/ml (Table 1). This is reminiscent of previous observations that the Δ*dltA* mutant was considerably more susceptible to cationic pore-forming antimicrobial peptides, such as nisin, α-defensins, and related peptides, than the wild-type strain is (32).

Analysis of transcriptional response pattern to chitosan. We carried out a genome-scale microarray experiment to detect global changes in *S. aureus* SG511 gene expression induced in response to treatment with a subinhibitory concentration of chitosan (15 μg/ml) for a short time (20 min), thereby identi-

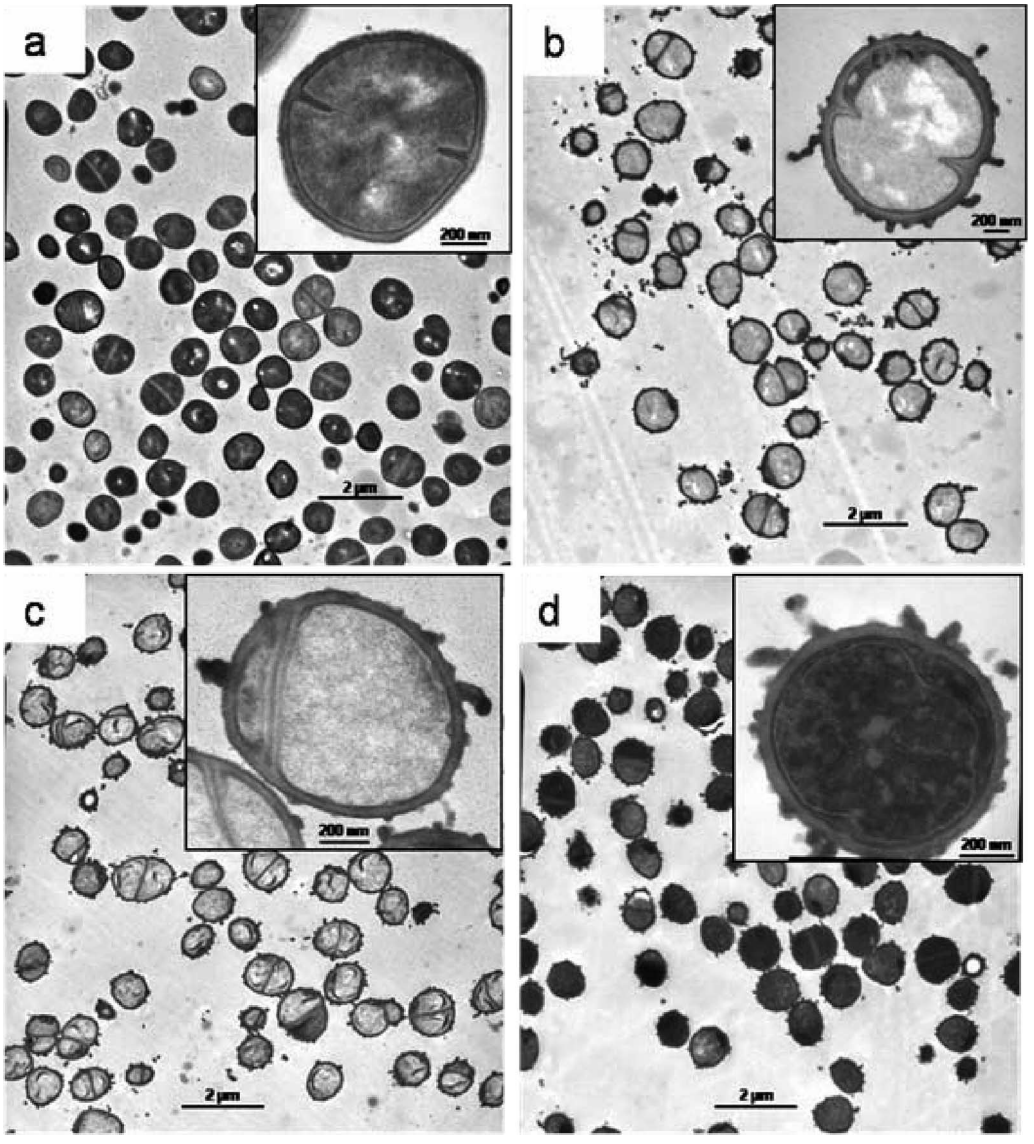

FIG. 4. Electron micrographs of *S. simulans* 22 cells (control) (a), treated with 10× MIC of chitosan for 5 min (b), 20 min (c), and 60 min (d). Insets show close-ups of single cells. Bars, 2 μm (panels a to d) and 200 nm (for insets of panels a to d).

fying fine-tuned responses of bacteria to the stress induced by chitosan. SAM (significance analysis of microarrays) revealed a total of 166 ORFs that showed a statistically significant change in expression level (with a 0.64% false discovery rate). A complete list of the significant gene responses, including 84 upregulated genes and 82 downregulated genes, is given in the supplemental material; Table 4 lists the most drastic changes, with a cutoff value arbitrarily set at twofold. Comparatively few changes in gene expression were observed upon chitosan treatment compared to cationic AMPs (31, 40).

Chitosan treatment reduced the bacterial growth rate, and this was clearly reflected in genetic expression profiles through the downregulation of macromolecular biosynthesis, including genes involved in RNA and protein synthesis (14 ribosomal protein genes), as well as in the metabolism of carbohydrates, amino acids, nucleotides, and nucleic acids (six genes), lipids, and coenzymes (Table 4).

Transcriptional response data provided us with indirect evidence that chitosan treatment interferes with cellular energy metabolism. This is supported by the fact that several of the genes preferentially expressed under oxygen depletion conditions were upregulated in this study. Under low-oxygen conditions and in the absence of external electron acceptors like oxygen or nitrate, NAD^+ is regenerated by fermentation or nitrate respiration, rather than through the respiratory chain (17). Among the proteins with the highest levels of transcription were enzymes of the fermentation pathways, including those coding for formate acetyltransferase (*pflB*), together with *pflA* (the activating enzyme), both catalyzing the nonoxidative transformation of pyruvate to acetyl coenzyme A and formate, and alcohol-acetaldehyde dehydrogenase (*adhE*), which corresponds to the typical response of a bacterium to oxygen-limiting conditions (17) and oxidative stress (8), as well as interruption of the electron transport chain (22). This is further

TABLE 4. Genes regulated in chitosan-treated *S. aureus* SG511 cells

ORF	Gene	Function[a]	Fold change[b]
Upregulated genes			
Membrane bioenergetics (electron transport chain and ATP synthase)			
SA0411	*ndhF*	NADH dehydrogenase subunit 5	2.2
SA2185	*narG*	Respiratory nitrate reductase alpha chain	2.2
Cell division			
SA0249	*scdA*	Cell division and morphogenesis-related protein	2.0
SA1023	*ftsL*	Cell division protein	2.8
Metabolism of carbohydrates and related molecules			
SA0143	*adhE*	Alcohol-acetaldehyde dehydrogenase	2.0
SA0218	*pflB*	Formate acetyltransferase	2.7
SA0219	*pflA*	Formate acetyltransferase-activating enzyme	6.4
Metabolism of amino acids and related molecules			
SA2189		HP, similar to NirR	2.5
Regulation of RNA synthesis			
SA1947	*czrA*	Repressor protein	2.0
Protein folding			
SA1659	*prsA*	Peptidyl-prolyl *cis/trans* isomerase homolog	2.4
Adaptation to atypical conditions			
SA1146	*bsaA*	Glutathione peroxidase	2.4
SA2405	*betA*	Choline dehydrogenase	2.1
Phage-related functions			
SA0252	*lrgA*	Holin-like protein LrgA	4.0
SA0253	*lrgB*	Holin-like protein LrgB	2.6
SA0754		HP, similar to lactococcal prophage ps3 protein 05	3.9
Miscellaneous			
SA0914		HP, similar to chitinase B	2.4
Hypothetical proteins			
SA0772		Conserved HP	3.6
SA0890		Conserved HP	2.0
SA1942		Conserved HP	2.6
SA0536		HP	2.7
SA1162		HP	2.0
SA1476		HP	3.1
SA1665		HP	2.5
SA2049		HP	2.7
SA2491		Conserved HP	2.1
SA2221		HP	2.8
SA2268		HP	2.6
Downregulated genes			
Transport/binding proteins and lipoproteins			
SA0952	*potC*	Spermidine/putrescine ABC transporter homolog	2.0
Metabolism of nucleotides and nucleic acids			
SA0920	*purQ*	Phosphoribosylformylglycinamidine synthase I PurQ	2.3
SA0921	*purL*	Phosphoribosylformylglycinamidine synthetase PurL	2.0
Metabolism of lipids			
SA0224		HP, similar to 3-hydroxyacyl-CoA dehydrogenase	2.4
SA0225		HP, similar to glutaryl-CoA dehydrogenase	2.4
Hypothetical proteins			
SA2050		Conserved HP	2.1

[a] HP, hypothetical protein; CoA, coenzyme A.
[b] Threshold ratio value set at ≥2.0-fold change.

substantiated by the fact that transcripts of the *nar* (*narG* and *narK*) and *nir* (SA2189) operons, involved in nitrite reduction and anaerobic respiration, a gene encoding a putative L-lactate permease (SA2156), the regulatory gene *srrA*, already shown to be involved in oxygen regulation in *S. aureus*, together with the gene *ndhF*, encoding an NADH dehydrogenase and linked to electron transport (17), were all found to be upregulated during chitosan treatment. Therefore, it appears reasonable to hypothesize that the electron transport chain was uncoupled in *S. aureus* SG511, resulting in impairment of oxygen consumption in response to chitosan treatment, which forced the bacteria to shift to anaerobic respiration.

Defects in menadione biosynthesis (such as in the case of SCV) result in interruptions in electron transport and decreased ATP production, thus inducing the expression of fermentation enzymes, even under aerobic conditions. This is an indication that, other than the oxygen concentration, several factors might act as a signal for anaerobic gene regulation in *S. aureus*, such as the reduced state of a component(s) of the respiratory chain, the membrane potential, and/or the increased level of NADH.

Acid stress is not likely to play a major role in chitosan's mode of action, since none of the urease genes, deemed to be an important acid shock mechanism for *S. aureus* to counteract

the acidic environment (6), was upregulated upon chitosan treatment. In addition, at relevant concentrations, the pH of the chitosan solution used was around neutrality.

None of the major peptidoglycan biosynthesis genes was regulated upon chitosan treatment. However, upregulated genes included *bsaA* and *prsA* and genes encoding the hypothetical proteins SA1703 and SA2221 which were also identified upon vancomycin treatment and which are considered parts of the staphylococcal cell wall stress stimulon (27, 45).

An operon encoding two potential membrane-associated proteins, designated LrgA and LrgB, is believed to confer negative control on extracellular murein hydrolase activity, by acting as "antiholins," thus inhibiting autolysis (18). Whereas Weinrick et al. showed that both genes were downregulated in mild acidic conditions (49), we saw that both genes were strongly upregulated under chitosan stress, which is in agreement with our electron micrographs, where no cell lysis could be observed.

The overall transcriptional profile of chitosan-treated *S. aureus* did not coincide with other published antibiotic profiles or with our own unpublished data file (mainly including cationic AMPs [31, 40]), indicating that chitosan's mode of action is difficult to compare with that of classical antimicrobials. Moreover, among the 166 genes that showed a statistically significant change in expression level, 32 (19.3%) encode enzymes of unknown specificity, 23 (13.9%) encode proteins of unknown function, and 46 (27.7%) encode hypothetical proteins, i.e., a total of 101 out of 166 genes (60.8%) are of unspecified function. This demonstrates the complexity of such an analysis and its limitations.

DISCUSSION

Different theories have been put forward to explain chitosan's antimicrobial mode of action. Some of the published papers, including that of Rabea et al. (35), fostered the impression that chitosan might have intracellular targets, such as DNA. Because of its cationic nature, chitosan has been widely investigated for the purpose of nonviral gene delivery in the form of DNA-chitosan complexes or as nanoparticles (7). However, the biological significance of this property is unclear, since chitosan would not normally be able to reach a cytoplasmic target, unless it is able to circumvent the plasma membrane.

The chelating activity of chitosan has often been implicated as a possible mode of action (35). Yet, based on our results, chelation of metals does not seem to be of importance for the antibiotic activity of chitosan; in contrast, the formation of complexes with metal ions appears to abrogate this activity.

The most prominent commercial use of chitosan is as a fat binder in dietary preparations (53). Wydro et al. demonstrated that there are significant electrostatic and hydrophobic interactions, as well as hydrogen bonds between lipids and chitosan (52). Related to this is the question of whether chitosan, being a lipid binder, might be able to extract lipids from the bacterial membrane. In view of the data we have gathered so far, this notion might be plausible, should there be sites on the cell surface where chitosan might interact with lipids extending from the membrane. However, we would have expected to observe a destabilization of liposomes upon contact with chitosan, which was not the case.

At present, the prevailing contention is that chitosan acts as a membrane perturbant (19, 21, 54). On the basis of the results discussed in this paper, we believe that such an activity might be part of its antibiotic mechanism. However, there is no evidence that chitosan's antimicrobial activity is mediated by a direct action on the cell membrane, because chitosan must first pass through the bacterial cell wall, composed of multilayers of cross-linked murein, to reach the plasma membrane. Various models have been proposed to predict the spatial arrangement of murein in the cell wall (11, 16, 47), all agreeing that the bacterial surface, including the peptidoglycan, must be porous, to allow the controlled ingress and egress of solutes. Pore sizes differed among the various models, ranging from 2.06 to 3 nm (47) up to 7 nm (16). Chitosan, being a linear polysaccharide, would have a diameter of around 1.1 nm in its extended conformation (11). One might hypothesize that chitosan would be able, at least in part, to diffuse through the pores in the murein structure. However, this seems unlikely in light of the fact that chitosan most probably exists in solution in a hydrated form that is much larger. Indeed, the hydrodynamic radius R_h of chitosan, which indicates the apparent size of the dynamic hydrated particle, was 24.59 nm $\pm$ 1.4 relative standard deviation (%) (Table 2). Therefore, none of the models of peptidoglycan structure would explain how a molecule with this size might be able to cross the cell wall. Moreover, there is no evidence that chitosan is broken down by extracellular staphylococcal enzymes into active smaller fragments which might pass through the cell wall more easily. In addition, dialyzed chitosan was fully antimicrobial, suggesting that large molecules are responsible for its activity.

Although chitosan and cationic AMPs share similar effects on treated cells on the cellular level, including cellular leakage and membrane perturbation, the transcriptional response patterns of both show surprisingly little similarity (31, 40). The upregulation of anaerobic pathways and the lack of interference in cell wall stress stimulon upon chitosan treatment suggest that the underlying antimicrobial mechanisms are different.

Transmission electron microscopy analysis of *S. simulans* 22 cells was consistent with an intact membrane but impaired membrane function. Shrinking of the membrane suggested water and ion loss from the cell. Yet the addition of chitosan to the growth medium was not likely to change osmotic conditions directly, instead it was inducing the leakage of ions (potassium, for instance) by an unknown mechanism, possibly by escaping through deenergetized K^+ transporters. No gross membrane disruption or pore formation was observed. Also, it appears unlikely that the changes in membrane permeability result from osmotic stress, since transcription of genes typically upregulated under such stress conditions, e.g., those responsible for accumulating proline and betaine (PutP, BPI, and BPII) (29), was not significantly altered after chitosan addition. Therefore, osmotic stress seems to be a result of chitosan's action, not its cause.

On the basis of our findings and the supporting literature, we believe that chitosan's mode of action is not confined to a single target molecule but that killing results from a sequence

of rather "untargeted" molecular events, taking place simultaneously or successively.

Our data clearly indicate that the initial contact between the polycationic chitosan macromolecule and the negatively charged cell wall polymers is indeed driven by electrostatic interactions and that teichoic acids play a major role (as seen with the *dltA* mutant, showing maximum susceptibility to chitosan), leading to a disruption of the equilibrium of cell wall dynamics. The originality of this hypothesis lies in the fact that the bacterial cell wall biogenesis is dynamic, with 40 to 45% of its structure released and recycled during each growth cycle (16). Although the possibility that dealanylated teichoic acids might represent a "target" for chitosan's action might spring to mind, we can, at this stage, neither explicitly refute nor confirm this contention. However, taking into account that the concentration of LTA in the outer leaflet of the cytoplasmic membrane of *S. aureus* is 10 to 20 mol% of polar lipids (15), a possible immobilization or even extraction of LTA by chitosan may have drastic consequences on the vital lateral diffusion of proteins as well as molecular machineries located within the cell membrane. Thus, LTA might provide a molecular link for chitosan at the cell surface, allowing it to disturb membrane functions.

Binding of chitosan to cell wall polymers would then trigger secondary cellular effects: destabilization and subsequent disruption of bacterial membrane function occur, albeit via unknown mechanisms, compromising the membrane barrier function and leading to leakage of cellular components without causing distinct pore formation. In addition, membrane-bound energy generation pathways are affected, probably due to impairment of the proper functional organization of the electron transport chain, thus interfering with proper oxygen reduction and forcing the cells to shift to anaerobic energy production. This might ultimately lead to dysfunction of the whole cellular apparatus. We may also tentatively speculate that the accumulation of the polymer in the membrane vicinity triggers various stress responses due to a local low pH or other factors that remain to be identified.

Nevertheless, the complex mechanisms by which these processes are coupled or interrelated have not been fully ascertained. Future work should aim at clarifying the molecular details of the underlying mechanisms and their relevance to the antimicrobial activity of chitosan. Moreover, further investigations in this area, in particular with regard to bacterial resistance mechanisms against this compound, are warranted.

ACKNOWLEDGMENTS

A Ph.D. scholarship granted to D.R. by the German Academic Exchange Service (DAAD) is gratefully acknowledged. Financial support was provided by the BONFOR program of the Medical Faculty, University of Bonn (to H.-G.S.), and the Deutsche Forschungsgemeinschaft (grant SFB670 to A.H.). K.V.B. is a recipient of a German National Foundation fellowship.

We are indebted to Mirko Weinhold (University of Bremen, Germany) for molecular weight and degree of deacetylation determinations. We are also very grateful to Andreas Peschel (University of Tübingen, Germany) for providing us with the *S. aureus* SA113 strains. The help of Vera Sass with the analysis of the microarray data is appreciated.

REFERENCES

1. **Babel, S., and T. A. Kurniawan.** 2003. Low-cost adsorbents for heavy metals uptake from contaminated water: a review. J. Hazard. Mater. **97:**219–243.
2. **Baumert, N., C. von Eiff, F. Schaaff, G. Peters, R. A. Proctor, and H.-G. Sahl.** 2002. Physiology and antibiotic susceptibility of *Staphylococcus aureus* small colony variants. Microb. Drug Resist. **8:**253–260.
3. **Bhatia, S. C., and N. Ravi.** 2003. A Mössbauer study of the interaction of chitosan and D-glucosamine with iron and its relevance to other metalloenzymes. Biomacromolecules **4:**723–727.
4. **Bierbaum, G., and H. G. Sahl.** 1987. Autolytic system of *Staphylococcus simulans* 22: influence of cationic peptides on activity of *N*-acetylmuramoyl-L-alanine amidase. J. Bacteriol. **169:**5452–5458.
5. **Bonelli, R. R., T. Schneider, H.-G. Sahl, and I. Wiedemann.** 2006. Insights into in vivo activities of lantibiotics from gallidermin and epidermin mode-of-action studies. Antimicrob. Agents Chemother. **50:**1449–1457.
6. **Bore, E., S. Langsrud, Ø. Langsrud, T. M. Rode, and A. Holck.** 2007. Acid-shock responses in *Staphylococcus aureus* investigated by global gene expression analysis. Microbiology **153:**2289–2303.
7. **Bowman, K., and K. W. Leong.** 2006. Chitosan nanoparticles for oral drug and gene delivery. Int. J. Nanomedicine **1:**117–128.
8. **Chang, W., D. A. Small, F. Toghrol, and W. E. Bentley.** 2006. Global transcriptome analysis of *Staphylococcus aureus* response to hydrogen peroxide. J. Bacteriol. **188:**1648–1659.
9. **Chirkov, S. N.** 2002. The antiviral activity of chitosan. Appl. Biochem. Microbiol. **38:**1–8. (In Russian.)
10. **Didenko, L. V., D. V. Gerasimenko, N. D. Konstantinova, T. A. Silkina, I. D. Avdienko, G. E. Bannikova, and V. P. Varlamov.** 2005. Ultrastructural study of chitosan effects on Klebsiella and staphylococci. Bull. Exp. Biol. Med. **140:**356–360.
11. **Dmitriev, B. A., F. V. Toukach, O. Holst, E. T. Rietschel, and S. Ehlers.** 2004. Tertiary structure of *Staphylococcus aureus* cell wall murein. J. Bacteriol. **186:**7141–7148.
12. **Doares, S. H., T. Syrovets, E. W. Weiler, and C. A. Ryan.** 1995. Oligogalacturonides and chitosan activate plant defensive genes through the octadecanoid pathway. Proc. Natl. Acad. Sci. USA **92:**4095–4098.
13. **Dodane, V., and V. D. Vilivalam.** 1998. Pharmaceutical applications of chitosan. Pharm. Sci. Technol. Today **1:**246–253.
14. **Fedtke, I., D. Mader, T. Kohler, H. Moll, G. Nicholson, R. Biswas, K. Henseler, F. Götz, U. Zähringer, and A. Peschel.** 2007. A *Staphylococcus aureus ypfP* mutant with strongly reduced lipoteichoic acid (LTA) content: LTA governs bacterial surface properties and autolysin activity. Mol. Microbiol. **65:**1078–1091.
15. **Fischer, W.** 1994. Lipoteichoic acid and lipids in the membrane of *Staphylococcus aureus*. Med. Microbiol. Immunol. **183:**61–76.
16. **Fisher, J. F., S. O. Meroueh, and S. Mobashery.** 2006. Nanomolecular and supramolecular paths toward peptidoglycan structure. Microbe **1:**420–427.
17. **Fuchs, S., J. Pané-Farré, C. Kohler, M. Hecker, and S. Engelmann.** 2007. Anaerobic gene expression in *Staphylococcus aureus*. J. Bacteriol. **189:**4275–4289.
18. **Groicher, K. H., B. A. Firek, D. F. Fujimoto, and K. W. Bayles.** 2000. The *Staphylococcus aureus lrgAB* operon modulates murein hydrolase activity and penicillin tolerance. J. Bacteriol. **182:**1794–1801.
19. **Helander, I. M., E.-L. Nurmiaho-Lassila, R. Ahvenainen, J. Rhoades, and S. Roller.** 2001. Chitosan disrupts the barrier properties of the outer membrane of Gram-negative bacteria. Int. J. Food Microbiol. **71:**235–244.
20. **Illum, L.** 1998. Chitosan and its use as a pharmaceutical excipient. Pharm. Res. **15:**1326–1331.
21. **Je, J.-Y., and S.-K. Kim.** 2006. Chitosan derivatives killed bacteria by disrupting the outer and inner membrane. J. Agric. Food Chem. **54:**6629–6633.
22. **Kohler, C., C. von Eiff, G. Peters, R. A. Proctor, M. Hecker, and S. Engelmann.** 2003. Physiological characterization of a heme-deficient mutant of *Staphylococcus aureus* by a proteomic approach. J. Bacteriol. **185:**6928–6937.
23. **Kuroda, M., T. Ohta, I. Uchiyama, T. Baba, H. Yuzawa, I. Kobayashi, L. Cui, A. Oguchi, K. Aoki, Y. Nagai, J. Q. Lian, T. Ito, M. Kanamori, H. Matsumaru, A. Maruyama, H. Murakami, A. Hosoyama, Y. Mizutani-Ui, N. K. Takahashi, T. Sawano, R. Inoue, C. Kaito, K. Sekimizu, H. Hirakawa, S. Kuhara, S. Goto, J. Yabuzaki, M. Kanehisa, A. Yamashita, K. Oshima, K. Furuya, C. Yoshino, T. Shiba, M. Hattori, N. Ogasawara, H. Hayashi, and K. Hiramatsu.** 2001. Whole genome sequencing of meticillin-resistant *Staphylococcus aureus*. Lancet **357:**1225–1240.
24. **Laemmli, U. K.** 1970. Cleavage of structural proteins during the assembly of the head of bacteriophage T4. Nature **227:**680–685.
25. **Lowry, O. H., N. J. Rosebrough, A. L. Farr, and R. J. Randall.** 1951. Protein measurement with the Folin phenol reagent. J. Biol. Chem. **193:**265–275.
26. **Lührmann, A., and A. Haas.** 2000. A method to purify bacteria-containing phagosomes from infected macrophages. Methods Cell Sci. **22:**329–341.
27. **McAleese, F., S. W. Wu, K. Sieradzki, P. Dunman, E. Murphy, S. Projan, and A. Tomasz.** 2006. Overexpression of genes of the cell wall stimulon in clinical isolates of *Staphylococcus aureus* exhibiting vancomycin-intermediate-*S. aureus*-type resistance to vancomycin. J. Bacteriol. **188:**1120–1133.
28. **Muzzarelli, R., R. Tarsi, O. Filippini, E. Giovanetti, G. Biagini, and P. E. Varaldo.** 1990. Antimicrobial properties of *N*-carboxybutyl chitosan. Antimicrob. Agents Chemother. **34:**2019–2023.
29. **O'Byrne, C. P., and I. R. Booth.** 2002. Osmoregulation and its importance to food-borne microorganisms. Int. J. Food Microbiol. **74:**203–216.

30. **Orlov, D. S., T. Nguyen, and R. I. Lehrer.** 2002. Potassium release, a useful tool for studying antimicrobial peptides. J. Microbiol. Methods **49:**325–328.
31. **Pag, U., M. Oedenkoven, V. Sass, Y. Shai, O. Shamova, N. Antcheva, A. Tossi, and H.-G. Sahl.** 2008. Analysis of *in vitro* activities and modes of action of synthetic antimicrobial peptides derived from an α-helical 'sequence template'. J. Antimicrob. Chemother. **61:**341–352.
32. **Peschel, A., M. Otto, R. W. Jack, H. Kalbacher, G. Jung, and F. Götz.** 1999. Inactivation of the *dlt* operon in *Staphylococcus aureus* confers sensitivity to defensins, protegrins, and other antimicrobial peptides. J. Biol. Chem. **274:** 8405–8410.
33. **Peter, M. G.** 1997. Introductory remarks. Carb. Eur. **19:**9–15.
34. **Proctor, R. A., C. von Eiff, B. C. Kahl, K. Becker, P. McNamara, M. Herrmann, and G. Peters.** 2006. Small colony variants: a pathogenic form of bacteria that facilitates persistent and recurrent infections. Nat. Rev. Microbiol. **4:**295–305.
35. **Rabea, E. I., M. E.-T. Badawy, C. V. Stevens, G. Smagghe, and W. Steurbaut.** 2003. Chitosan as antimicrobial agent: applications and mode of action. Biomacromolecules **4:**1457–1465.
36. **Rhoades, J., and S. Roller.** 2000. Antimicrobial actions of degraded and native chitosan against spoilage organisms in laboratory media and foods. Appl. Environ. Microbiol. **66:**80–86.
37. **Rouget, M. C.** 1859. Des substances amylacées dans les tissus des animaux, spécialement des Articulés (chitine). Comp. Rend. **48:**792–795.
38. **Ruhr, E., and H.-G. Sahl.** 1985. Mode of action of the peptide antibiotic nisin and influence on the membrane potential of whole cells and on cytoplasmic and artificial membrane vesicles. Antimicrob. Agents Chemother. **27:**841–845.
39. **Sahl, H.-G., U. Pag, S. Bonness, S. Wagner, N. Antcheva, and A. Tossi.** 2005. Mammalian defensins: structures and mechanism of antibiotic activity. J. Leukoc. Biol. **77:**466–475.
40. **Sass, V., U. Pag, A. Tossi, G. Bierbaum, and H.-G. Sahl.** Mode of action of human β-defensin 3 against *Staphylococcus aureus* and transcriptional analysis of responses to defensin challenge. Int. J. Med. Microbiol. doi:10.1016/j.ijmm.2008.01.011.
41. **Singla, A. K., and M. Chawla.** 2001. Chitosan: some pharmaceutical and biological aspects—an update. J. Pharm. Pharmacol. **53:**1047–1067.
42. **Takai, K., T. Ohtsuka, Y. Senda, M. Nakao, K. Yamamoto, J. Matsuoka, and Y. Hirai.** 2002. Antibacterial properties of antimicrobial-finished textile products. Microbiol. Immunol. **46:**75–81.
43. **Tharanathan, R. N., and F. S. Kittur.** 2003. Chitin—the undisputed biomolecule of great potential. Crit. Rev. Food Sci. Nutr. **43:**61–87.
44. **Ueno, H., T. Mori, and T. Fujinaga.** 2001. Topical formulations and wound healing applications of chitosan. Adv. Drug Deliv. Rev. **52:**105–115.
45. **Utaida, S., P. M. Dunman, D. Macapagal, E. Murphy, S. J. Projan, V. K. Singh, R. K. Jayaswal, and B. J. Wilkinson.** 2003. Genome-wide transcriptional profiling of the response of *Staphylococcus aureus* to cell-wall-active antibiotics reveals a cell-wall-stress stimulon. Microbiology **149:**2719–2732.
46. **van de Rijn, I., and R. E. Kessler.** 1980. Growth characteristics of group A streptococci in a new chemically defined medium. Infect. Immun. **27:**444–448.
47. **Vollmer, W., and J. V. Holtje.** 2004. The architecture of the murein (peptidoglycan) in gram-negative bacteria: vertical scaffold or horizontal layer(s)? J. Bacteriol. **186:**5978–5987.
48. **Weidenmaier, C., J. F. Kokai-Kun, S. A. Kristian, T. Chanturiya, H. Kalbacher, M. Gross, G. Nicholson, B. Neumeister, J. J. Mond, and A. Peschel.** 2004. Role of teichoic acids in *Staphylococcus aureus* nasal colonization, a major risk factor in nosocomial infections. Nat. Med. **10:**243–245.
49. **Weinrick, B., P. M. Dunman, F. McAleese, E. Murphy, S. J. Projan, Y. Fang, and R. P. Novick.** 2004. Effect of mild acid on gene expression in *Staphylococcus aureus*. J. Bacteriol. **186:**8407–8423.
50. **Wiedemann, I., R. Benz, and H.-G. Sahl.** 2004. Lipid II-mediated pore formation by the peptide antibiotic nisin: a black lipid membrane study. J. Bacteriol. **186:**3259–3261.
51. **Wiedemann, I., E. Breukink, C. van Kraaij, O. P. Kuipers, G. Bierbaum, B. de Kruijff, and H.-G. Sahl.** 2001. Specific binding of nisin to the peptidoglycan precursor lipid II combines pore formation and inhibition of cell wall biosynthesis for potent antibiotic activity. J. Biol. Chem. **276:**1772–1779.
52. **Wydro, P., B. Krajewska, and K. Hąc-Wydro.** 2007. Chitosan as a lipid binder: a Langmuir monolayer study of chitosan-lipid interactions. Biomacromolecules **8:**2611–2617.
53. **Ylitalo, R., S. Lehtinen, E. Wuolijoki, P. Ylitalo, and T. Lehtimäki.** 2002. Cholesterol-lowering properties and safety of chitosan. Arzneimittelforschung **52:**1–7. (In German.)
54. **Zakrzewska, A., A. Boorsma, S. Brul, K. J. Hellingwerf, and F. M. Klis.** 2005. Transcriptional response of *Saccharomyces cerevisiae* to the plasma membrane-perturbing compound chitosan. Eukaryot. Cell **4:**703–715.